# Smad7 binds differently to individual and tandem WW3 and WW4 domains of WWP2 ubiquitin ligase isoforms

**Lloyd C. Wahl[1, #], Jessica E. Watt[1, §], Hiu T. T. Yim[1], Danielle De Bourcier[2], James Tolchard[2, ¶], Surinder M. Soond[1, ✦], Tharin M. A. Blumenschein[2*], and Andrew Chantry[1*]**

[1] From the School of Biological Sciences, University of East Anglia, Norwich NR4 7TJ, UK
[2] From the School of Chemistry, University of East Anglia, Norwich NR4 7TJ, UK
[#] Present address: Department of Infectious Diseases and Public Health, Jockey Club College of Veterinary Medicine and Life Sciences, City University of Hong Kong, Hong Kong
[§] Present Address: Northern Institute for Cancer Research, Newcastle University, Newcastle upon Tyne NE2 4HH, UK
[¶] Present Address: EMBL-EBI, Wellcome Genome Campus, Hinxton, Cambridgeshire, CB10 1SD, UK.
[✦] Present Address: Institute of Molecular Medicine, Sechenov First Moscow State Medical University, Trubetskaya str. 8-2, 119991, Moscow, Russian Federation.
[*] Correspondence: a.chantry@uea.ac.uk
[*] Correspondence: t.blumenschein@uea.ac.uk

**Keywords:** Smad, E3 ubiquitin ligase, WW domain, Smad7, TGFβ signalling, NEDD4, protein interaction

# Supplementary Material

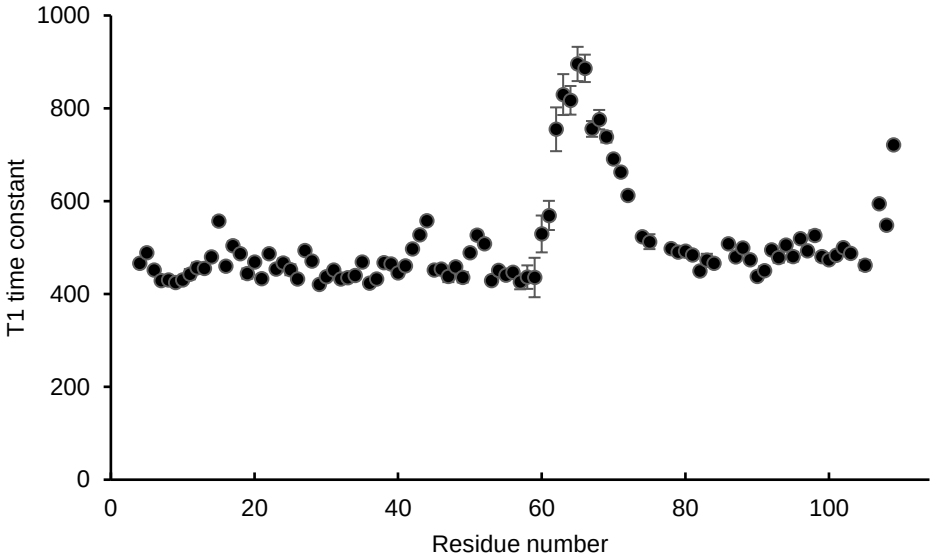


**Figure S1**. (**A**) Backbone amide $T_1$ relaxation constants for residues of the GB1-WW4 construct. GB1: residues 1-61, Linker: residues 62-66, WW4: residues 67-114.

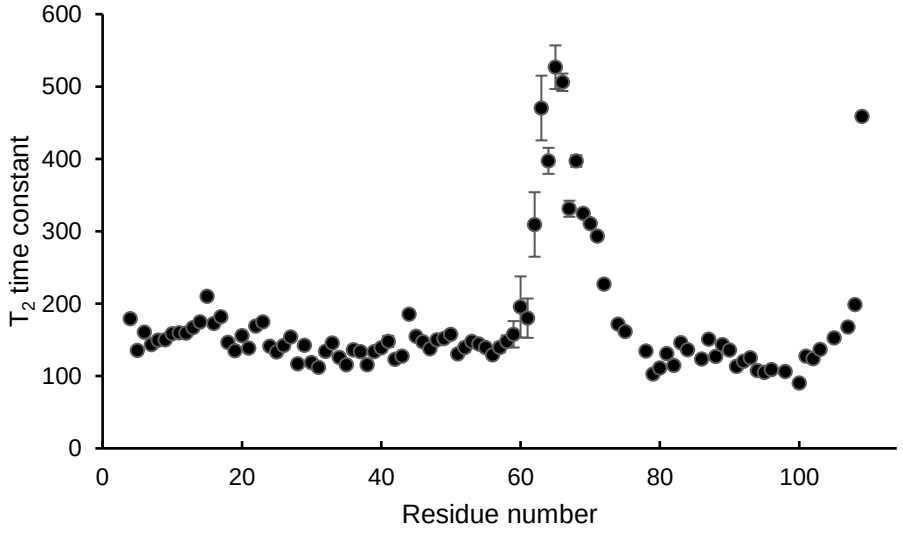


**Figure S1.** (**B**) Backbone amide $T_2$ relaxation constants for residues of the GB1-WW4 construct. GB1: residues 1-61, Linker: residues 62-66, WW4: residues 67-114.

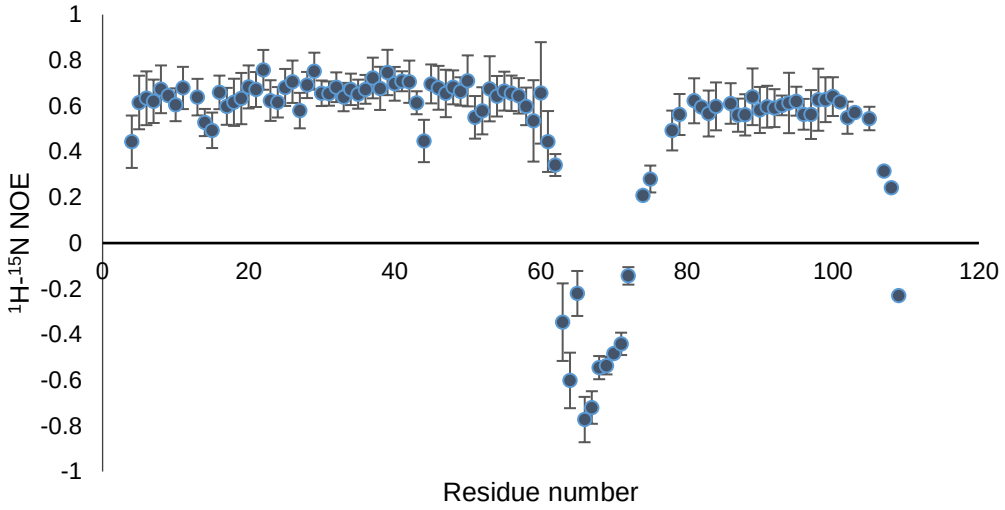


**Figure S1.** (**C**) Backbone amide $^{1}H$-$^{15}N$ NOE relaxation for residues of the GB1-WW4 construct. GB1: residues 1-66, Linker: residues 62-66, WW4: residues 67-114.

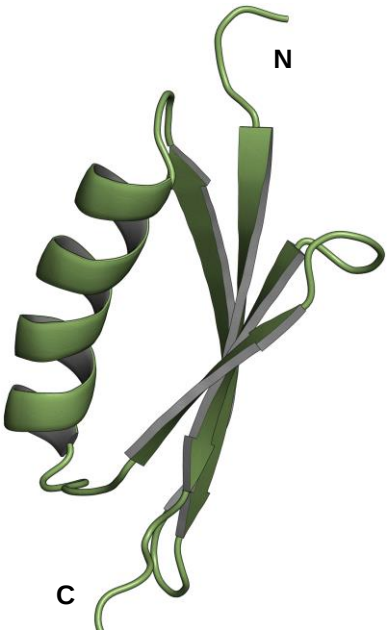


**Figure S2** (**A**) Ribbon diagram depiction of the GB1 tag from the most representative model (model 16) of the refined 20-model structural ensemble.

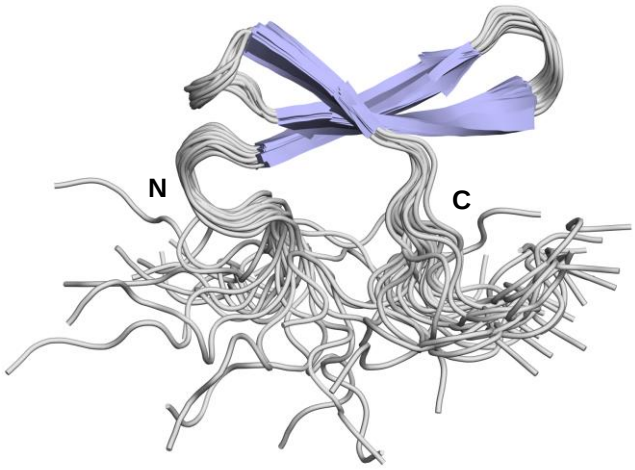


**Figure S2.** (**B**) Ribbon diagram depiction of the refined 20-model WW4 domain structural ensemble.

**Table S1.** Clustal Omega [1] alignment of NEDD4 WW domains. (An asterisk indicates fully conserved residues. A colon indicates residues with strongly similar properties. A full stop indicates weakly similar properties.)

| | Domain sequence | Similarity (%) |
|---|---|---|
| **WWP2 WW4** | PALPPGWEMKYTSEGVRYFVDHNTRTTTFKDPRP | 100 |
| **WWP1 WW4** | EPLPEGWEIRYTREGVRYFVDHNTRTTTFKDPRN | 79.41 |
| **HECW2 WW2** | LELPRGWEMKHDHQGKAFFVDHNSRTTTFIDPRL | 61.76 |
| **SMURF1 WW2** | GPLPPGWEVRSTVSGRIYFVDHNNRTTQFTDPRL | 61.76 |
| **SMURF2 WW3** | GPLPPGWEIRNTATGRVYFVDHNNRTTQFTDPRL | 61.76 |
| **ITCH WW4** | KPLPEGWEMRFTVDGIPYFVDHNRRTTTYIDPRT | 61.76 |
| **NEDD4L WW3** | SFLPPGWEMRIAPNGRPFFIDHNTKTTTWEDPRL | 55.88 |
| **HECW1 WW2** | LELPRGWEIKTDQQGKSFFVDHNSRATTFIDPRI | 55.88 |
| **ITCH WW3** | GPLPPGWEKRTDSNGRVYFVNHNTRITQWEDPRS | 55.88 |
| **WWP2 WW3** | GPLPPGWEKRQD-NGRVYYVNHNTRTTQWEDPRT | 54.55 |
| **WWP1 WW3** | GPLPPGWEKRVDSTDRVYFVNHNTKTTQWEDPRT | 52.94 |
| **NEDD4 WW2** | SGLPPGWEEKQDERGRSYYVDHNSRTTTWTKPTV | 52.94 |
| **WWP2 WW2** | RPLPPGWEKRTDPRGRFYYVDHNTRTTTWQRPTA | 52.94 |
| **WWP2 WW1** | DALPAGWEQRELPNGRVYYVDHNTKTTTWERPLP | 52.94 |
| **WWP1 WW1** | ETLPSGWEQRKDPHGRTYYVDHNTRTTTWERPQP | 52.94 |
| **NEDD4 WW3** | GFLPKGWEVRHAPNGRPFFIDHNTKTTTWEDPRL | 50 |
| **ITCH WW2** | EPLPPGWERRVDNMGRIYYVDHFTRTTTWQRPTL | 50 |
| **WWP1 WW2** | QPLPPGWERRVDDRRRVYYVDHNTRTTTWQRPTM | 50 |
| **NEDD4L WW1** | PPLPPGWEEKVDNLGRTYYVNHNNRTTQWHRPSL | 50 |
| **HECW2 WW1** | EALPPNWEARIDSHGRIFYVDHVNRTTTWQRPTA | 47.06 |
| **NEDD4L WW2** | PGLPSGWEERKDAKGRTYYVNHNNRTTTWTRPIM | 47.06 |
| **HECW1 WW1** | EPLPPNWEARIDSHGRVFYVDHVNRTTTWQRPTA | 44.12 |
| **ITCH_WW1** | APLPPGWEQRVDQHGRVYYVDHVEKRTTWDRPEP | 44.12 |
| **NEDD4 WW1** | SPLPPGWEERQDILGRTYYVNHESRRTQWKRPTP | 44.12 |
| **SMURF1 WW1** | PELPEGYEQRTTVQGQVYFLHTQTGVSTWHDPRI | 41.18 |
| **SMURF2 WW2** | PDLPEGYEQRTTQQGQVYFLHTQTGVSTWHDPRV | 41.18 |
| **NEDD4L WW4** | GPLPPGWEERIHLDGRTFYIDHNSKITQWEDPRL | 41.18 |
| **NEDD4 WW4** | GPLPPGWEERTHTDGRIFYINHNIKRTQWEDPRL | 38.24 |
| **SMURF2 WW1** | NDLPDGWEERRTASGRIQYLNHITRTTQWERPTR | 38.24 |
| | ** .:* :  ::.  : :  * | |

**Table S2.** GPS 3.0 phosphorylation prediction [2] at S206 of human Smad7.

| | Position | Context | Score | Cutoff | Kinase | Prediction |
|---|---|---|---|---|---|---|
| Smad7 | 206 | SRLCELESPPPPYSR | 23.412 | 6.118 | CMGC/MAPK/JNK/JNK2 | YES |
| Smad7 | 206 | SRLCELESPPPPYSR | 17.346 | 7.867 | CMGC/CDK/CDK5/CDK5 | YES |
| Smad7 | 206 | SRLCELESPPPPYSR | 15.278 | 9.411 | CMGC/CDK/CDK2/CDC28 | YES |
| Smad7 | 206 | SRLCELESPPPPYSR | 13.243 | 4.61 | CMGC/MAPK/ERK/Erk2 | YES |
| Smad7 | 206 | SRLCELESPPPPYSR | 12.722 | 8.145 | Atypical/PIKK/FRAP | YES |
| Smad7 | 206 | SRLCELESPPPPYSR | 12.625 | 10.326 | CMGC/MAPK/ERK/Erk1 | YES |
| Smad7 | 206 | SRLCELESPPPPYSR | 12.062 | 6.781 | CMGC/MAPK/JNK/JNK3 | YES |
| Smad7 | 206 | SRLCELESPPPPYSR | 11.898 | 4.168 | CMGC/CDK/CDC2/CDK1 | YES |
| Smad7 | 206 | SRLCELESPPPPYSR | 11.263 | 6.616 | CMGC/CDK/CDK5 | YES |
| Smad7 | 206 | SRLCELESPPPPYSR | 10.833 | 7.061 | CMGC/CDK/CDK5/PHO85 | YES |
| Smad7 | 206 | SRLCELESPPPPYSR | 10.667 | 3.833 | CMGC/MAPK/ERK/FUS3 | YES |
| Smad7 | 206 | SRLCELESPPPPYSR | 10.143 | 3.221 | CMGC/CDK/CRK7 | YES |
| Smad7 | 206 | SRLCELESPPPPYSR | 10.143 | 3.221 | CMGC/CDK/CRK7/CRK7 | YES |
| Smad7 | 206 | SRLCELESPPPPYSR | 10.03 | 4.309 | CMGC/MAPK/p38 | YES |
| Smad7 | 206 | SRLCELESPPPPYSR | 8.971 | 4.55 | CMGC/MAPK | YES |
| Smad7 | 206 | SRLCELESPPPPYSR | 8.2 | 7.46 | CMGC/MAPK/p38/HOG1 | YES |
| Smad7 | 206 | SRLCELESPPPPYSR | 8.192 | 4.698 | CMGC/CDK/CDC2 | YES |
| Smad7 | 206 | SRLCELESPPPPYSR | 8.094 | 6.826 | CMGC/CDK/CDK2/CDK2 | YES |
| Smad7 | 206 | SRLCELESPPPPYSR | 8 | 4.95 | CAMK/CAMKL/AMPK/AMPKA2 | YES |
| Smad7 | 206 | SRLCELESPPPPYSR | 7.667 | 6.008 | Other/Other-Unique/KIS | YES |
| Smad7 | 206 | SRLCELESPPPPYSR | 6.404 | 3.933 | CMGC/CDK | YES |
| Smad7 | 206 | SRLCELESPPPPYSR | 6.403 | 4.507 | CMGC/DYRK | YES |
| Smad7 | 206 | SRLCELESPPPPYSR | 6.333 | 4.25 | AGC/PKA/PKACB | YES |
| Smad7 | 206 | SRLCELESPPPPYSR | 6.333 | 5.7 | CMGC/MAPK/ERK/Erk4 | YES |
| Smad7 | 206 | SRLCELESPPPPYSR | 6.333 | 3.483 | Other/NEK/NEK11/NEK11 | YES |
| Smad7 | 206 | SRLCELESPPPPYSR | 5.828 | 3.205 | Atypical/PIKK/FRAP/MTOR | YES |
| Smad7 | 206 | SRLCELESPPPPYSR | 5.824 | 2.841 | CMGC/GSK/GSK3A | YES |
| Smad7 | 206 | SRLCELESPPPPYSR | 5.741 | 5.425 | CMGC/MAPK/p38/MAPK11 | YES |
| Smad7 | 206 | SRLCELESPPPPYSR | 5.667 | 4 | Other/MOS | YES |
| Smad7 | 206 | SRLCELESPPPPYSR | 5.667 | 4 | Other/MOS/MOS | YES |
| Smad7 | 206 | SRLCELESPPPPYSR | 5.5 | 5.133 | CK1/TTBK/TTBK1 | YES |
| Smad7 | 206 | SRLCELESPPPPYSR | 4.706 | 3.307 | CMGC/CDK/CDK4/CDK4 | YES |
| Smad7 | 206 | SRLCELESPPPPYSR | 4.704 | 3.279 | CMGC/DYRK/DYRK1 | YES |
| Smad7 | 206 | SRLCELESPPPPYSR | 4.445 | 4.186 | Atypical/PIKK | YES |
| Smad7 | 206 | SRLCELESPPPPYSR | 4.019 | 1.106 | AGC/PDK1 | YES |
| Smad7 | 206 | SRLCELESPPPPYSR | 3.612 | 2.944 | CMGC/MAPK/JNK | YES |
| Smad7 | 206 | SRLCELESPPPPYSR | 3.331 | 1.667 | CMGC/MAPK/ERK | YES |
| Smad7 | 206 | SRLCELESPPPPYSR | 2.469 | 0.899 | AGC/PDK1/PDPK1 | YES |
| Smad7 | 206 | SRLCELESPPPPYSR | 2.446 | 2.107 | CMGC/MAPK/p38/MAPK14 | YES |
| Smad7 | 206 | SRLCELESPPPPYSR | 2.137 | 1.892 | CMGC/MAPK/JNK/JNK1 | YES |
| Smad7 | 206 | SRLCELESPPPPYSR | 2.13 | 2.07 | CMGC | YES |
| Smad7 | 206 | SRLCELESPPPPYSR | 1.704 | 1.499 | CMGC/CDK/CDK2 | YES |
| Smad7 | 206 | SRLCELESPPPPYSR | 1.515 | 0.897 | CMGC/DYRK/HIPK | YES |
| Smad7 | 206 | SRLCELESPPPPYSR | 1.5 | 0.3 | CMGC/MAPK/ERK/Erk3 | YES |
| Smad7 | 206 | SRLCELESPPPPYSR | 1.379 | 1.199 | CMGC/DYRK/HIPK/HIPK2 | YES |
| Smad7 | 206 | SRLCELESPPPPYSR | 0.242 | 0.213 | CMGC/CDK/CDK7/CDK7 | YES |
| Smad7 | 206 | SRLCELESPPPPYSR | 0 | 0 | TKL/RIPK | . |

**Table S3**. NetPhos 3.1 phosphorylation prediction [3,4] at S206 of human Smad7.

| | Position | Context | Score | Cutoff | Kinase | Prediction |
|---|---|---|---|---|---|---|
| Smad7 | 206 | CELESPPPP | 0.614 | 0.5 | cdk5 | YES |
| Smad7 | 206 | CELESPPPP | 0.519 | 0.5 | cdc2 | YES |
| Smad7 | 206 | CELESPPPP | 0.51 | 0.5 | GSK3 | YES |
| Smad7 | 206 | CELESPPPP | 0.484 | 0.5 | p38MAPK | . |
| Smad7 | 206 | CELESPPPP | 0.444 | 0.5 | CaM-II | . |
| Smad7 | 206 | CELESPPPP | 0.368 | 0.5 | CKI | . |
| Smad7 | 206 | CELESPPPP | 0.353 | 0.5 | DNAPK | . |
| Smad7 | 206 | CELESPPPP | 0.304 | 0.5 | CKII | . |
| Smad7 | 206 | CELESPPPP | 0.302 | 0.5 | ATM | . |
| Smad7 | 206 | CELESPPPP | 0.296 | 0.5 | RSK | . |
| Smad7 | 206 | CELESPPPP | 0.287 | 0.5 | PKG | . |
| Smad7 | 206 | CELESPPPP | 0.106 | 0.5 | PKA | . |
| Smad7 | 206 | CELESPPPP | 0.092 | 0.5 | PKB | . |
| Smad7 | 206 | CELESPPPP | 0.066 | 0.5 | unsp | . |
| Smad7 | 206 | CELESPPPP | 0.053 | 0.5 | PKC | . |

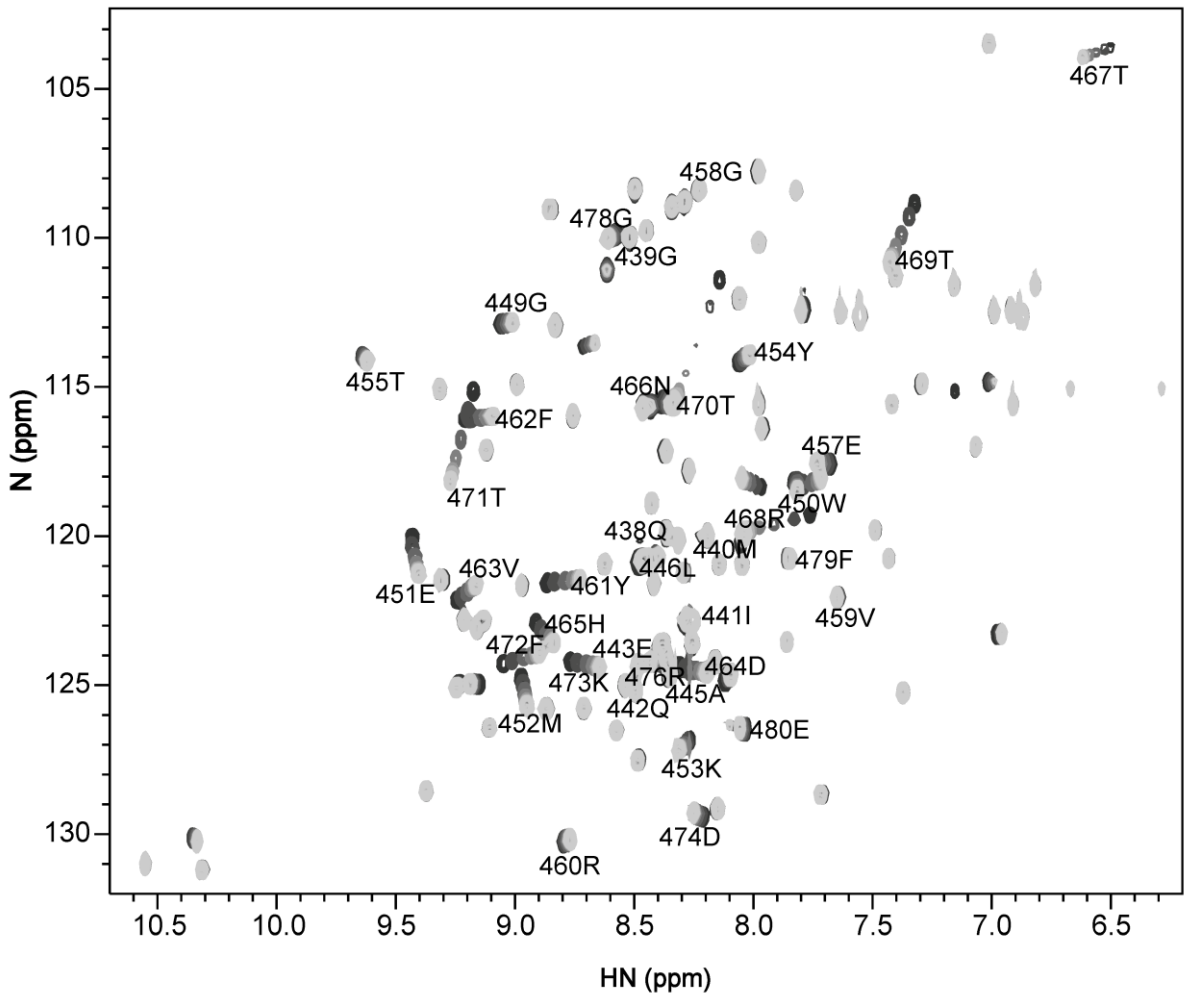


**Figure S3.** (**A**) The superimposed WW4/Smad7 titration HSQCs. Lower ligand concentrations are in light grey and higher ligand concentrations are in dark grey.

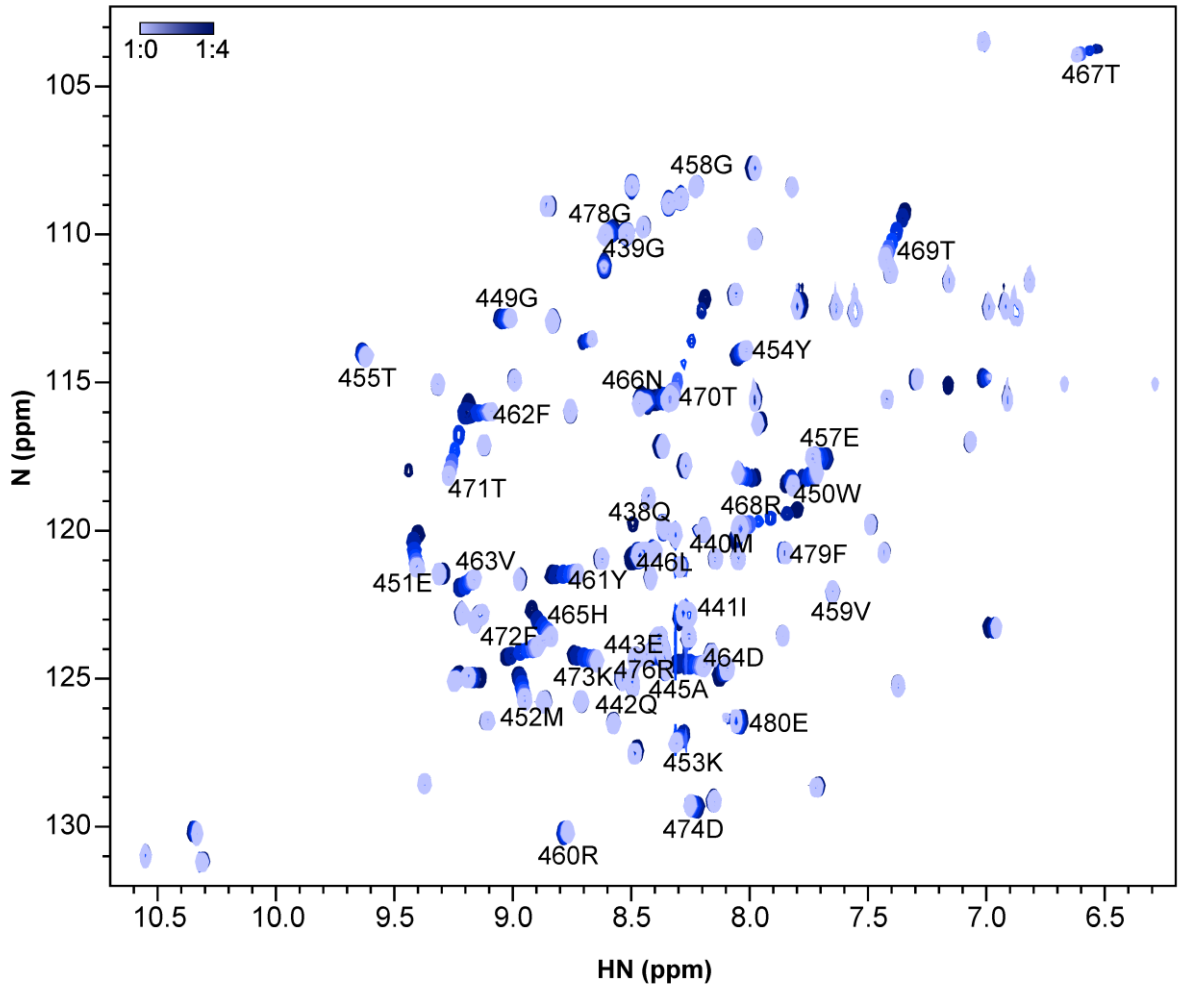


**Figure S3.** (**B**) The superimposed WW4/pSmad7 titration HSQCs. Lower ligand concentrations are in light blue and higher ligand concentrations are in dark blue.

5′- GCAGTCCTGTTTATGTTTCAAAACTATATACATATGACTTCGGGCCGGGTGCAGGG
GCTCACACCTGTAATCCTAGCACTTTGGGAGGCTGAGGCGAGAGGATTGCTTGAGCCCAG
GAGTTTGAGACTAGCCTGAGCCACACGGGGAGGCTTCCATGTCTACAAAAATTTTTTTAA
AAAATTAGTTGAATGTGATGGTGCATTCCTGTGGTCCTAGCTATTCAGGAGGCTAAGGTG
GGAGGATCACTTGAGCCTGGGAGGTGAGGCTGCAGTGAGCCATGATCCTGCTACTCTACT
CTAGCCTGGACTAACAGAGTGAGACCCTGTCAAAAAAAAAAAAAAATCTTTGGTAACAAA
AATAAATAAAAATCACTAGTTTAGACAAATTATGAGAAAGCTAGGAAGGTTCCAGATTTT
TGTGAGCCTTGTGTACTTACTAAAGGATTTTGACTCAAGGGCAATGGGGAGTCAATGGAA
GTGTTGTTGTTGTTGTTGTTGTTTGAGACAGGATCTCACTCTGTCGCCCAGGCTGGA
ATGTAGCAGCATAATCATAGTTCACTGTAGCCTTGATCTCCCAGGCACAAGCAGTCCTCC
CACCTCAGCTGCCCAAGTAGCTGGGACCAAGGGCGCACACTCCACCACCCCCAGCTAATT
TTTAAAAAATATTTTTGTAGAGATGGGGGTCTCCCTCTGTTGCTTAGGCTGGTCAATTGA
AGTTTTTGAGCAGGAGTGTGACCGAAGGGCTCAGTCTAGTGGGTTACTCTGATGGCTATT
TGTAGGCTGGATGGAGTGGGGAGGTTAATTCTGGGGTAGGAGCAGTAGTCCAGGGGTGAG
GTGATACAGATCTGGACATAGGAATGGAAAATGGAAAGTCAGTGGCAGGGAGACTGAAAA
AGCAGCAGTCAGGCTGAATGATTGATAGCAGCGGGAATGATGTTGGCCTGGTTTCATCCC
TGGGAGGAGAATTGACATGAGGAGACTGAAGAAAGGCCTGGGTGTGGGGAGAGAGCTGTG
GCATTCAATTGAATGAAGGGTGACAGCTGGTCATGAAGGTGAGGCACTCTAGCAGGCAGA
ATCCAGACAAAATCTGGGAACTGACTGTGGGTCCTAGGAACCACTTGAGGGGAAACCATT
TTTAGGGAGGCCTTGAGTTTAAAAAAAAATCATTGAGGCCGGGTGCAGTGGCTCACGCCT
GTAATCTCAGCACTTTGGGAGGCCGAGGTGGGAGGATCGTTTGAGTCCAGGAGTTCGAGA
CCAGTCTGGGCAACATGGCGAAACTCCATCTCTACTAAAAATATAAACAGTGAGACTCTG
TCTCAAAACAAAACAAAACCAAAGACCATGCAACATGTTTACACTGGCACCTTATATCAG
GTGAGTTTCAGTTGCAAGTAACAAAAGTTGTTAGCAACATTGGCTTAAATAAGGAAGGGA
ATGTATTGGCTCATGTAACTGAAAATTCTAGATATCAATCCTGATTCCAAGCGAAGCTTG
GGCTACTCAACAATATCACCAAGGAATTGGCTTTCTCCCATTTTTCTGCTCTGCCATCC
ACTGGGTCAACTTCCTATTGTCTTCGGGTCCAAAATAATAGCCAGTGGCCCCCAGGACCA
CATGCTTCCTCAGTCATATTCAGAAAGGATGAGCAACTATTATTTTTCCTAGATTTGCTA
GCAGATGTCCTGAGATTGGCTGTGGCTGGCTCAACATACATCACATGTGCACTTCTGGTC
CAGGCAACCATGCAACTCTGAGGTTGGGAACAGAGTCAGCTTCCCCAGAACCACATGGAT
CCCCAAATTAGAAATTGAGAGCTAATGGCAAGGAGGGATTGGGTGCTGCAGAGGCAACCA
CAGATGTCTGCTATAATCAGCTAAGCCCCAGCAACCTCTGTGACAGGGCCTGCCCGGCTG
TGCTAGGCATCCTGAGACTTTTCTAGAATTGGGGGATGGGAGTGGGGTGGTCATTATATT
CATTCTGAGGTTCCTATTTCCAG – 3′

**Figure S4.** (**A**) The nucleotide sequence of the predicted WWP2-ΔHECT promoter within intron 9/10. Putative AP-1, Smad [5] and SOX9 responsive elements highlighted in purple, cyan and yellow respectively. TATA boxes are highlighted in grey.

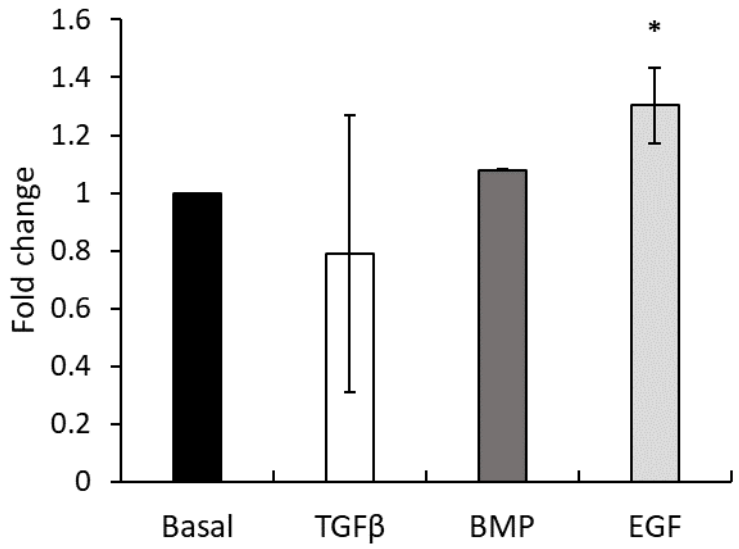


**Figure S4** (**B**) Luciferase activity of the prospective WWP2-ΔHECT 2 kb promoter region under different growth factor conditions in HEK293A cells

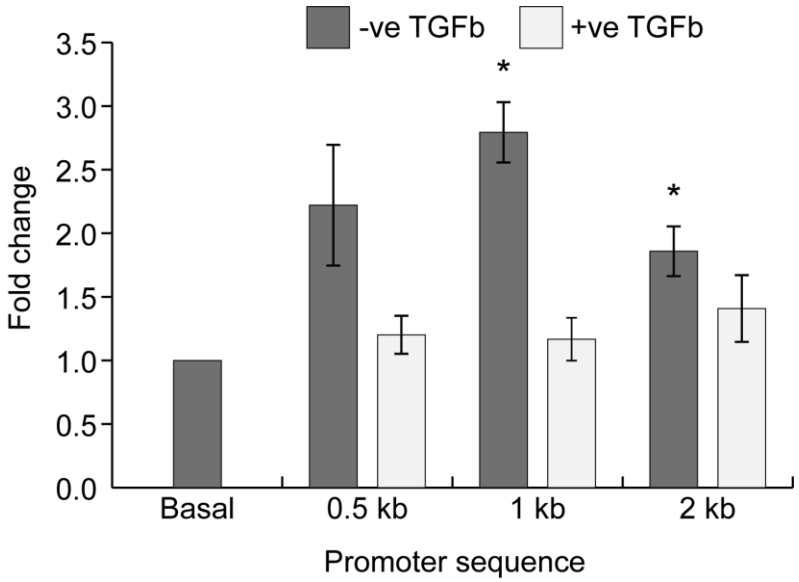


**Figure S4** (**C**) Luciferase activity of different regions of the prospective WWP2-ΔHECT promoter in HEK293A cells

Table S4 – Residues in intermediate exchange in WW3/Smad7 and WW3-4/Smad7 titrations

| *WW3-4/Smad7* | *WW3/Smad7* |
|---|---|
| 410Gly | 416Asp |
| 413Lys | 427Thr |
| 416Asp | 428Arg |
| 426Asn | 430Thr |
| 427Thr | 431Gln |
| 428Arg | 432Trp |
| 430Thr | 433Glu |
| 431Gln | |
| 432Trp | |
| 433Glu | |

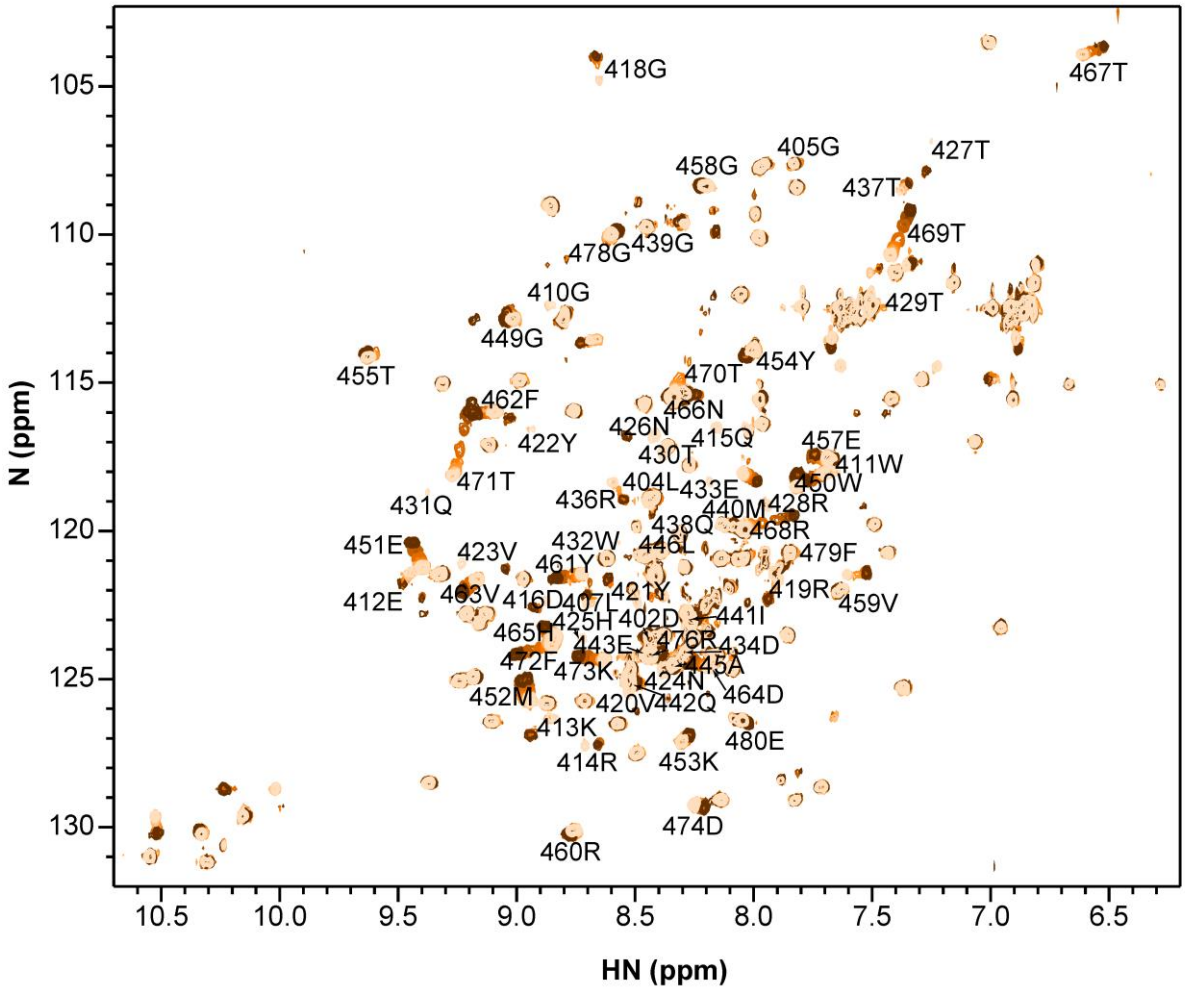


**Figure S5.** (**A**) The superimposed WW3-4/Smad7 titration HSQCs. Lower ligand concentrations are in light orange and higher ligand concentrations are in dark orange.

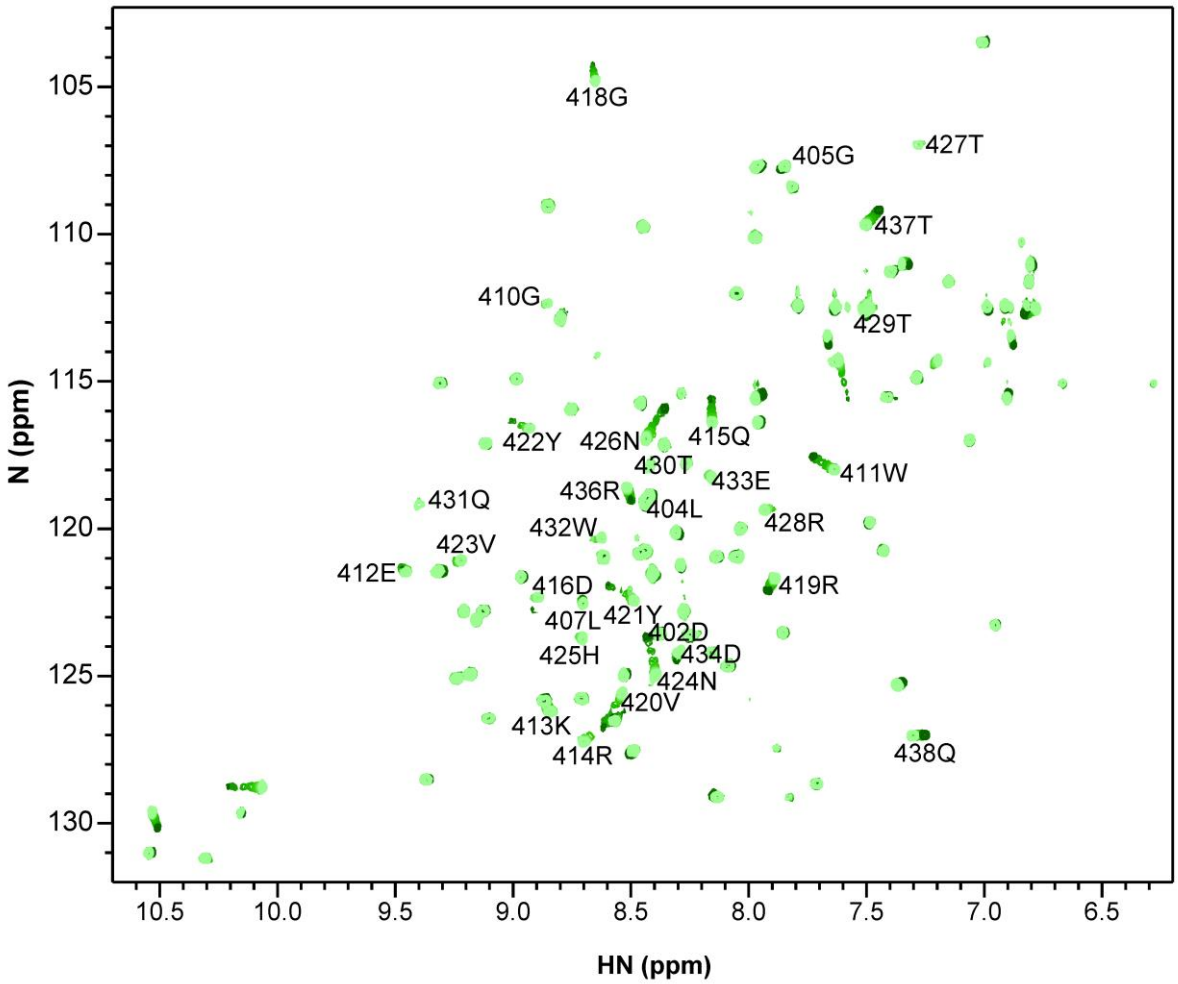


**Figure S5.** (**B**) The superimposed WW3/Smad7 titration HSQCs. Lower ligand concentrations are in light green and higher ligand concentrations are in dark green.

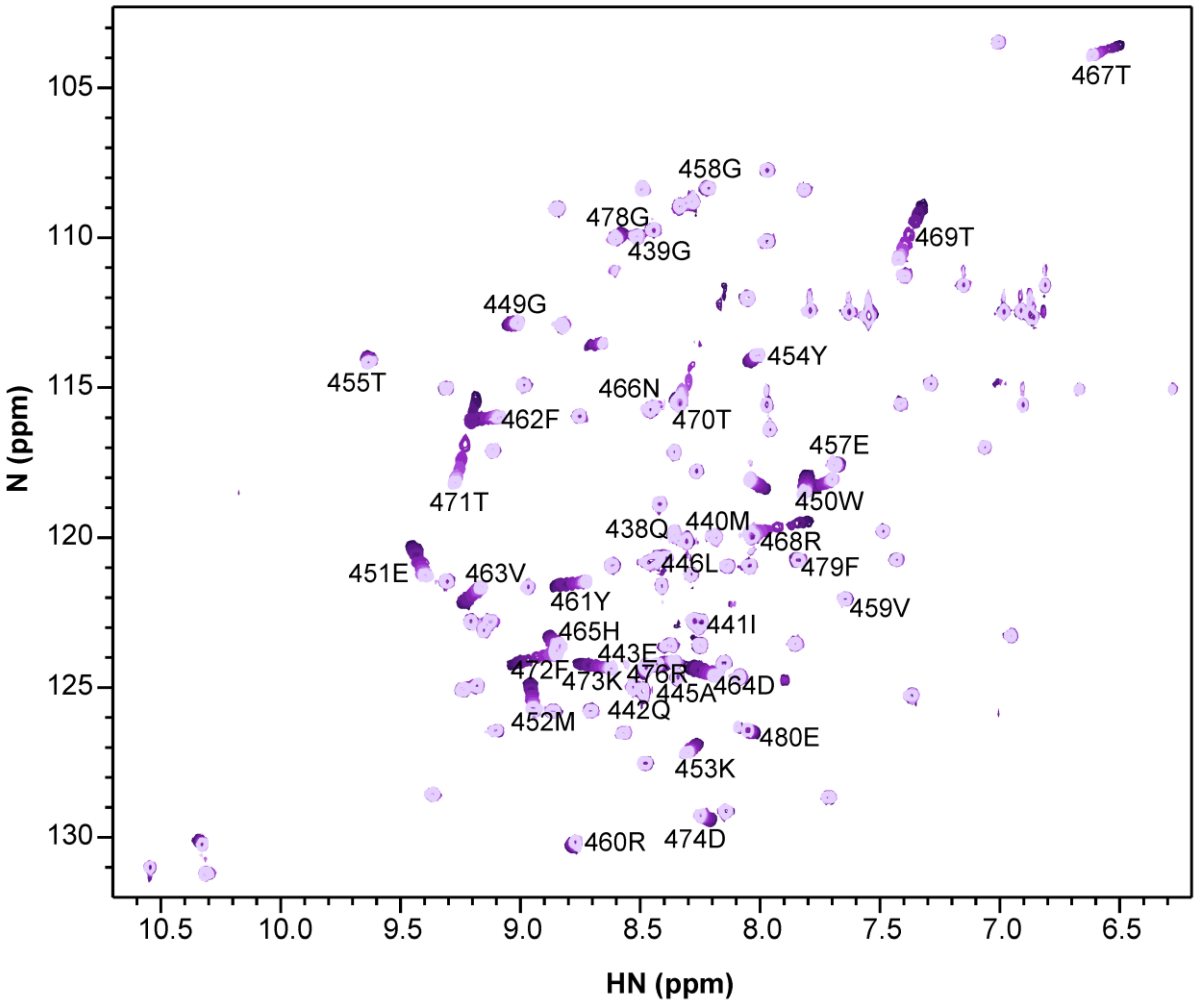


**Figure S5.** (**C**) The superimposed WW4/Smad7 titration HSQCs. Lower ligand concentrations are in light purple and higher ligand concentrations are in dark purple.

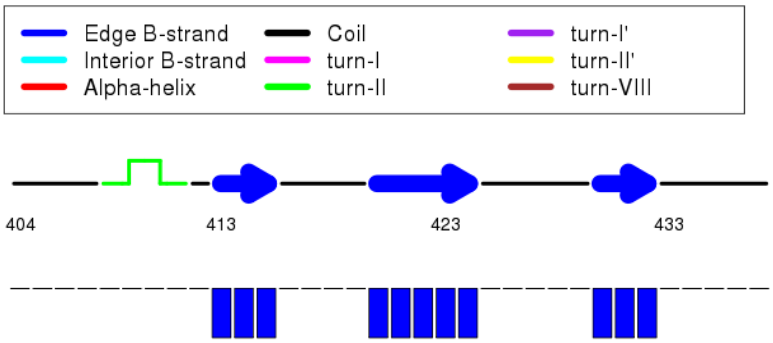


**Figure S5.** (**D**) The CSI 3.0 webserver [6] output predicting the secondary structure of WW3 based on backbone chemical shifts.

Table S5 – Acquisition parameters for the GB1-WW4 NMR spectra

| Spectrum | Scans | Complex points | | | Spectral width | | |
|---|---|---|---|---|---|---|---|
| | | $^{1}H$ | $^{15}N$ | $^{13}C$ | $^{1}H$ | $^{15}N$ | $^{13}C$ |
| $^{1}H$-$^{15}N$-HSQC | 8 | 1024 | 256 | - | 12019 | 2595 | - |
| $^{1}H$-$^{13}C$-HSQC | 64 | 1024 | - | 256 | 12019 | - | 16077 |
| CBCA(CO)NH | 24 | 1024 | 64 | 130 | 12019 | 2433 | 15105 |
| HNCACB | 24 | 1024 | 64 | 132 | 12019 | 2433 | 15105 |
| CC(CO)NH | 32 | 1024 | 42 | 128 | 12019 | 2433 | 15105 |
| H(CCO)NH | 48 | 1024 | 48 | 160 ($^{1}H$) | 12019 | 2433 | 11990 ($^{1}H$) |
| HCCH-TOCSY | 8 | 1024 | 120 ($^{1}H$) | 32 | 7507.5 | 6995.6 ($^{1}H$) | 9423.8 |
| CCH-TOCSY | 8 | 1024 | 120 ($^{13}C$) | 32 | 7507.5 | 9423.8 ($^{13}C$) | 9423.8 |
| HbCbCgCdHd | 256 | 1024 | - | 48 | 12820.5 | - | 6038.6 |
| Aromatic $^{13}C$ TOCSY | 32 | 1024 | - | 48 | 11160 | - | 2823 |
| Aromatic TROSY HSQC | 1024 | 1024 | - | 256 | 7212 | - | 8052 |
| Aromatic NOESY[1] | 16 | 1024 | 256 ($^{1}H$) | 0 | 12019 | 10395 ($^{1}H$) | 15105.7 |
| $^{15}N$-NOESY-HSQC | 32 | 1024 | 48 | 152($^{1}H$) | 7508 | 1519 | 6997 ($^{1}H$) |
| $^{13}C$-NOESY-HSQC | 16 | 1024 | 192 ($^{1}H$) | 64 | 11161 | 10395 ($^{1}H$) | 15105 |

[1](1H-1H 2D plane NOESY-HSQC @ 120 ppm for 13C)

Supplementary Methods

***NMR Spectroscopy***

$^{15}N$ $T_1$, $^{15}N$ $T_2$, and $^{1}H$-$^{15}N$ NOE backbone amide relaxation experiments [7] were acquired at 293 K with a Bruker Avance I 500 MHz NMR spectrometers and $^{15}N$-labelled GB1-WW4. $T_1$ measurements were performed with a 5 s recovery delay and relaxation delays of 0.02, 0.1, 0.2, 0.5, 0.75, 1, 2, and 4 s. The relaxation delays of 0.02, 0.5, and 1 s were repeated to evaluate data consistency. $T_2$ measurements were performed with a 5 s recovery delay and relaxation delays of 18, 53, 88, 141, 176, 211 and 263 ms. Relaxation delays of 18, 88 and 176 ms were repeated to evaluate data consistency. NOE measurements used a saturation delay of 5 s, replaced by a relaxation delay of 5 s in the reference experiment. NMR data were processed and analysed as described in the main text.

***Luciferase assay***

Constructs were made by cloning 2 kb, 1 kb or 0.5 kb of the same region of *wwp2* intron 19/20 into the pGL4.27 vector (Promega). HEK293A cells were transfected with either of these plasmids and the pSV-β-Galactosidase control vector (Promega). Cells were stimulated with TGFβ (5 ng $ml^{-1}$), BMP-4 (10 ng $ml^{-1}$) or EGF (10 ng $ml^{-1}$) and incubated overnight at 37°C, 5% $CO_2$. Luciferase activity was determined using the Promega Luciferase Assay System following the manufacturer's instructions. Data were normalised against β-galactosidase activity.

Supplementary References


1. Sievers, F.; Wilm, A.; Dineen, D.; Gibson, T.J.; Karplus, K.; Li, W.; Lopez, R.; McWilliam, H.; Remmert, M.; Söding, J.; et al. Fast, scalable generation of high-quality protein multiple sequence alignments using Clustal Omega. *Mol. Syst. Biol.* **2011**, *7*, 539.

2. Xue, Y.; Ren, J.; Gao, X.; Jin, C.; Wen, L.; Yao, X. GPS 2.0, a Tool to Predict Kinase-specific Phosphorylation Sites in Hierarchy. *Mol. Cell. Proteomics* **2008**, *7*, 1598–1608.

3. Blom, N.; Sicheritz-Pontén, T.; Gupta, R.; Gammeltoft, S.; Brunak, S. Prediction of post-translational glycosylation and phosphorylation of proteins from the amino acid sequence. *Proteomics* **2004**, *4*, 1633–1649.

4. Blom, N.; Gammeltoft, S.; Brunak, S. Sequence and structure-based prediction of eukaryotic protein phosphorylation sites. *J. Mol. Biol.* **1999**, *294*, 1351–1362.

5. Martin-Malpartida, P.; Batet, M.; Kaczmarska, Z.; Freier, R.; Gomes, T.; Aragón, E.; Zou, Y.; Wang, Q.; Xi, Q.; Ruiz, L.; et al. Structural basis for genome wide recognition of 5-bp GC motifs by SMAD transcription factors. *Nat. Commun.* **2017**, *8*, 2070.

6. Hafsa, N.E.; Arndt, D.; Wishart, D.S. CSI 3.0: a web server for identifying secondary and super-secondary structure in proteins using NMR chemical shifts. *Nucleic Acids Res.* **2015**, *43*, W370–W377.

7. Farrow, N.A.; Muhandiram, R.; Singer, A.U.; Pascal, S.M.; Kay, C.M.; Gish, G.; Shoelson, S.E.; Pawson, T.; Forman-Kay, J.D.; Kay, L.E. Backbone Dynamics of a Free and a Phosphopeptide-Complexed Src Homology 2 Domain Studied by 15N NMR Relaxation. *Biochemistry* **1994**, *33*, 5984–6003.